ChemPubSoc Europe

DOI: 10.1002/ejoc.201901058

EurJOC European Journal of Organic Chemistry

Full Paper

Cavitands in Catalysis

Evaluation of the Catalytic Capability of *cis*- and *trans*-Diquinoxaline Spanned Cavitands

Mami Inoue,[a] Shinsuke Kamiguchi,[a] Katto Ugawa,[a] Shaima Hkiri,[b,c] Jules Bouffard,[b] David Sémeril,*[b] and Tetsuo Iwasawa*[a]

Abstract: Three new *cis*-diquinoxaline spanned cavitands were successfully synthesized. These *cis*-diphosphinated derivatives were applied in homogeneous gold-catalyzed dimerization and hydration of alkynes as well as rhodium-catalyzed styrene hydroformylation. The results were ranked with those obtained with their *trans*-diphosphinated isomeric analogues. The structure-activity relationship employing these two cavitands reveals that the *cis*- or *trans*-positioning of the catalyst centers directly influences cooperation between the two metallic atoms to control catalytic activity, reaction profile, and product selectivity. This comparative study provides us an intellectual basis for future catalytic cavitand chemistry and homogeneous catalysis.

Introduction

Resorcin[4]arene-cavitand, able to carry out a catalytic reaction, is an important supramolecule that mimics enzymatic catalysis and achieves marvelous chemical transformations from the viewpoint of green chemistry.[1–3] The cavitands have strong resemblances in two points to natural enzymes: one, cavitands are partly open, guest substrates readily fill the space, enter and leave; the second, cavitands are endowed with gently curved concave large enough to accommodate catalytic centers. Despite the relevant role played by catalytic cavitands, such a class of cavitands is underrepresented owing to synthetic difficulties.[4,5] To make supramolecular cavitands those weigh over MW ca. 1000 preparatively in pure form is a basically embarrassing synthesis. When we attempt to introduce reactive centers inside the hydrophobic pockets, isomeric production of in- and outwardly oriented cavitands towards the pockets often occurs. Hence, we chemists are always struggling to understand even basic aspect of cavitand catalysis.[6] It might be quite a challenge for us to imitate enzymatic virtue that Mother Nature has meticulously created for more than long, long four billion years, because synthetic chemistry has been in just one or two hundred year-period history since Friedrich Wöhler synthesized urea from ammonium cyanate.[7,8]

Recently, we have developed for catalytic applications *trans*-di-quinoxaline-spanned resorcin[4]arenes.[9] An introverted bis-gold cavitand was efficient in the dimerization of two different terminal alkynes.[10] Another type of gold cavitand, in which a

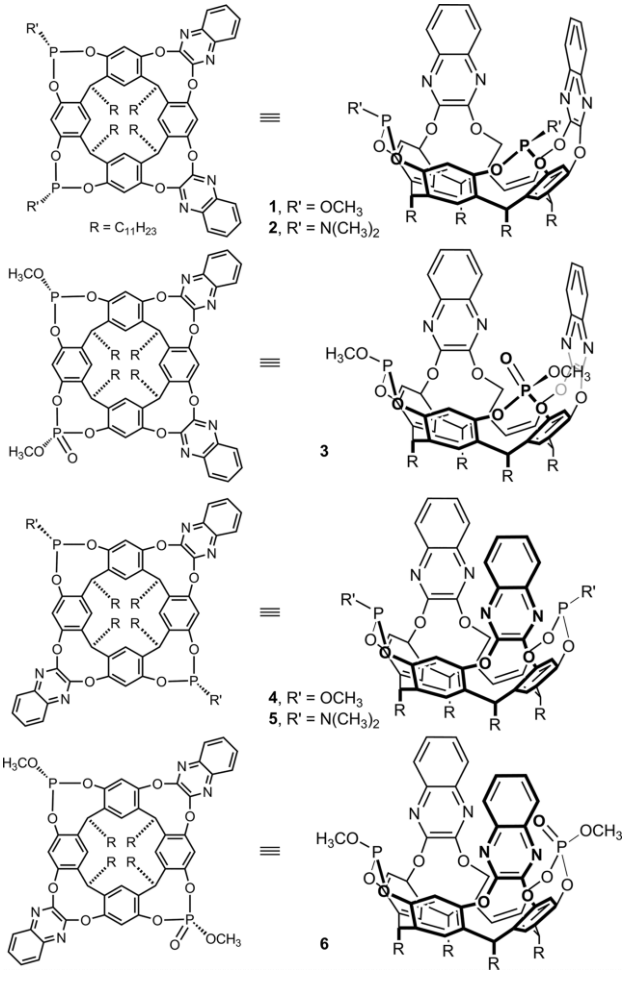

Figure 1. Diquinoxaline-spanned resorcin[4]arenes those are in *cis*-**1**, *cis*-**2** and *cis*-**3** and in *trans*-**4**, *trans*-**5** and *trans*-**6**.

[a] *Department of Materials Chemistry, Ryukoku University, Seta, Otsu, Shiga, 520-2194, Japan*
E-mail: iwasawa@rins.ryukoku.ac.jp
http://www.chem.ryukoku.ac.jp/iwasawa/index.html
[b] *Synthèse Organométallique et Catalyse, UMR-CNRS 7177, Université de Strasbourg, 4 rue Blaise Pascal, 67070 Strasbourg Cedex, France*
E-mail: dsemeril@unistra.fr
[c] *Faculté des Sciences de Bizerte, Université de Carthage, 7021 Jarzouna, Bizerte, Tunisia*

Supporting information and ORCID(s) from the author(s) for this article are available on the WWW under https://doi.org/10.1002/ejoc.201901058.

Lewis acid gold cation was associated to a Lewis basic P=O moiety, displayed high regio-selectivities in addition of H_2O to unsymmetrical alkynes; for example, 3-octanone was yielded in 91 % starting from 3-octyne.[11] Although the advantage of cavitand catalysis in selective transformations are obvious, yet a study of structure-activity relationship is not obvious enough. Particularly, from the viewpoint of basic research, comprehension of mechanistic aspects awaits upgrading. Herein we report a structure-activity relationship of phosphinated cavitands in transition metal-catalysis. We prepared new *cis*-type P(III) (**1** and **2**) and mixed P(III)/P(V) (**3**) extended cavitands, which are structurally similar to previously reported *trans*-type **4**, **5**, and **6** (Figure 1): those are used as ligands in gold- and rhodium-catalysis. The question we pursue here is *"How does the difference between these trans- and cis-arrangements affect the catalytic activity and selectivity?"*

Results and Discussion

We started to synthesize *cis*-**1** from a reaction between resorcin[4]arene and 2,3-dichloroquinoxaline (Scheme 1(a)). Preparation of *cis*-positioned di-quinoxaline-spanned resorcin[4]arene was laborious,[12] and the use of DABCO (1,4-diazabicyclo-[2.2.2]octane) and pyridine improved the chemical yield to 22 %. The obtained *cis*-positioned tetra-ol cavitand reacted with $P(OCH_3)_3$ to give two of the three possible isomers ("out-out", "in-out", and "in-in"). The two compounds were carefully separated by silica-gel column chromatography and were isolated in 44 % and 22 % yield for "out-out" **1** and "in-out" *iso*-**1**, respectively (Scheme 1(b)).[13] Orientation of the lone pair of the phosphorus atoms was deduced from their ^{1}H NMR spectra. In the case of **1**, its ^{1}H NMR spectrum reveals one doublet located at 3.87 ppm ($^3J_{PH}$ = 8.6 Hz) for the two "out-out" $POCH_3$ (Figure 2 (a)); in the spectrum of *iso*-**1**, two doublets at 3.87 ppm ($^3J_{PH}$ = 8.6 Hz) and at 3.20 ppm ($^3J_{PH}$ = 12.6 Hz), which can be attributed to the two kinds of "in-out" $POCH_3$ protons (Figure 2 (b)). The latter upfield-shifted doublet (δ = 3.20 ppm) results from anisotropic effects of the aromatic π clouds; thus, the OCH_3 group resides inside. Consequently, in cavitand **1**, the two $POCH_3$ moieties pointed outside: this was similar observation to previously reported cavitands **4** (δ = 3.97 ppm, $^3J_{PH}$ = 8.7 Hz, Figure 2 (c)) and *iso*-**4** in Figure 3 (δ = 3.98 ppm, $^3J_{PH}$ = 8.3 Hz and δ = 3.10 ppm, $^3J_{PH}$ = 12.4 Hz, Figure 2 (d)). Oxidation of only one phosphorus atom of **1** was carried out in the use of 1.0 equivalent mCPBA (*meta*-chloroperbenzoic acid), and **3** was isolated in 30 % yield (Scheme 1(c)).[14] The *cis*-tetra-ol platform also reacted with $P[N(CH_3)_2]_3$, and a mostly single spot on TLC was observed, and desired **2** was obtained in 40 % yield in pure form (Scheme 1(a)); in the ^{1}H NMR spectrum of **2**, there is one

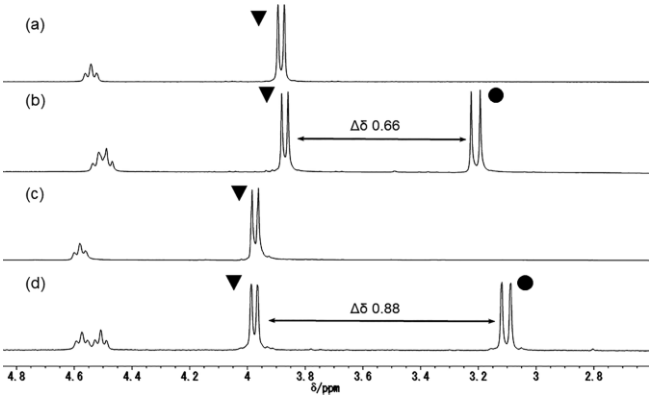

Figure 2. Portions of ^{1}H NMR spectra (400 MHz, $CDCl_3$) of (a) **1**, (b) *iso*-**1**, (c) **4**, (d) *iso*-**4**. The peaks labeled with circles and triangles correspond to inward- and outward-oriented $POCH_3$, respectively.

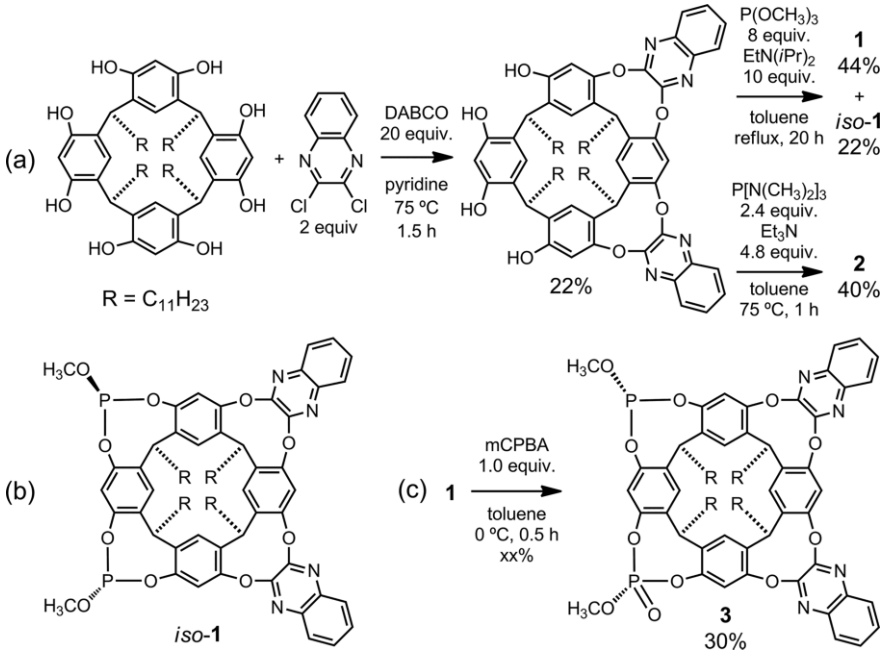

Scheme 1. (a) Synthesis of *cis*-**1** and *cis*-**2**; (b) *iso*-**1** bearing both inward- and outward $POCH_3$ groups; (c) synthesis of *cis*-**3** (mCPBA = *meta*-chloroperbenzoic acid).

doublet peak located at 2.76 ppm with $^3J_{PH}$ = 10.5 Hz that can be attributed to PN(CH_3)$_2$. As previously reported, we observed *trans*-**5** as a single isomer, due to steric reason, with similar 2.81 ppm with $^3J_{PH}$ = 10.5 Hz, and ensured that two PN(CH_3)$_2$ groups clearly point outside on the basis of crystallographic analysis; thus, two PN(CH_3)$_2$ bonds of *cis*-**2** were inferred to direct outwardly.[15]

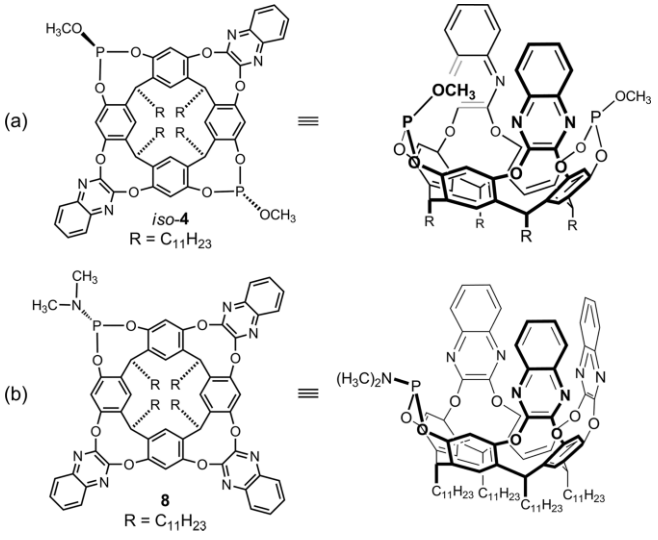

Figure 3. Structures of (a) *iso*-**4** that has both in- and outside P-OMe, and (b) mono-phosphoramidite **8** that was flanked by three quinoxalines.

The conformational flexibility of tetra-quinoxaline-spanned resorcin[4]arenes is well known, and can fluctuate between vase (close) and kite (open) conformations.[16] The conformation of the related cavitands is deduced from its ^{1}H NMR spectra, because the chemical shift of methine protons directly beneath quinoxaline moieties explains vase or kite form. A chemical shift at around 5.5 ppm indicates a vase conformer, whereas a chemical shift at ca. 3.7 ppm expresses a kite version. For our four new compounds (**1**, *iso*-**1**, **2** and **3**), ^{1}H NMR investigations carried out in $CDCl_3$ and [D_8]toluene, clearly indicate a vase conformation of the cavitands: the methine protons appear at 5.73 (**1**), 5.76 and 5.71 (*iso*-**1**), 5.70 (**2**), 5.79–5.71 (**3**) ppm in $CDCl_3$, and at 6.14 (**1**), 6.15 and 6.08 (*iso*-**1**), 6.15 (**2**) and 6.20 and 6.11 (**3**) ppm in [D_8]toluene. Then, we had an interest in the difference in π-clouded environment between *cis*- and *trans*-walled cavitands. For that, we compared the chemical shifts of the CH_3 proton of the $POCH_3$ moieties in cavitands *iso*-**1** and *iso*-**4**. As shown in Figure 2 (b) and (d), these $\Delta\delta$ (differences in the chemical shifts between inward- and outward-oriented $POCH_3$) are 0.66, and 0.88 for *iso*-**1** and *iso*-**4**, respectively. This result is important evidence suggesting that the *trans*-walls create a definite compartment that is more heavily influenced by the π-clouds than the compartment of the *cis*-walled cavitand.

Phosphites **1** and **3** readily formed complexes with AuCl•S(CH_3)$_2$. When Au/P ratios of 1.2:1 in toluene were used, *cis*-**1**•(AuCl)$_2$ and *cis*-**3**•AuCl complexes were isolated in quantitative and 63 % yields, respectively (Scheme 2). These gold complexes were tested in cross- and homo-dimerization of alkynes as well as in hydration of di-substituted alkynes. Their performances in catalysis will be ranking with the *trans*-**4**•(AuCl)$_2$ and *trans*-**6**•AuCl complexes.[9b,17]

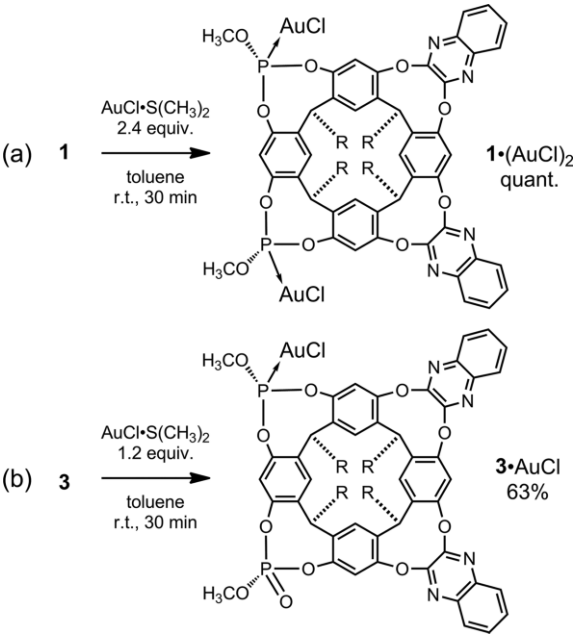

Scheme 2. Complexation between cavitands and AuCl•S(CH_3)$_2$ for synthesis of (a) **1**•(AuCl)$_2$, and (b) **3**•AuCl.

For the gold-catalyzed dimerization of terminal alkynes, the runs were carried out using 1 mol-% of *cis*-**1**•(AuCl)$_2$ or *trans*-**4**•(AuCl)$_2$ complex and 2 mol-% of AgOTf in toluene at room temperature (Scheme 3). In use of *cis*-**1**•(AuCl)$_2$ whether for cross-dimerization of ethynylbenzene and 1-octyne (in part (a)) or for homo-dimerization of 1-octyne (in part (b)), only 2-octanone (**7c**) that results from hydration of 1-octyne was observed in 29 % and 35 % yield, respectively. These results contrast with those observed when the tests were repeated using the *trans*-**4**•(AuCl)$_2$ complex. The *trans*-**4**•(AuCl)$_2$ formed only dimer products, with a ratio cross-**7a**/homo-**7b** = 75:25 (in part (a)) and with >99 % yield of **7b** (in part (b)). These results

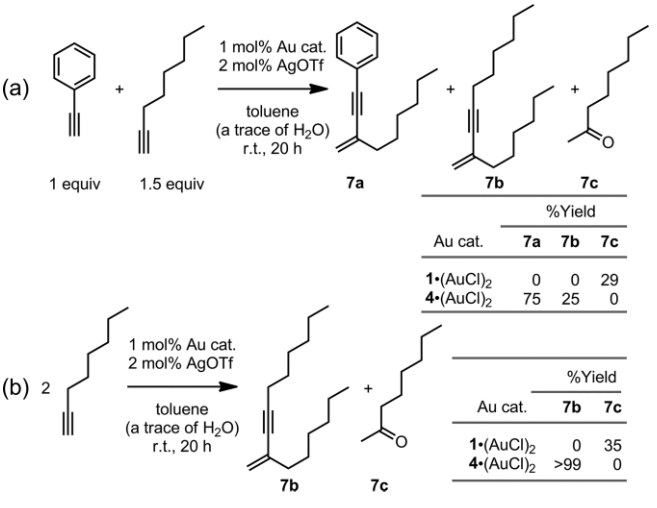

Scheme 3. Catalytic evaluation of *cis*-**1**•(AuCl)$_2$ and *trans*-**4**•(AuCl)$_2$ in (a) cross-dimerization, and (b) homo-dimerization.

clearly show the importance of the positioning of the two gold centers on the resorcin[4]arene skeleton. Different bis-gold complexes between *cis*- and *trans*-walled cavitands led to different type of active species and catalytic outcome. *Cis*-positioning phosphorus atoms led to a more open cavitands, which leads to a highly reactive species toward traces of water present in commercially available dry toluene.

Differences in activity and regioselectivity could also be highlighted in the gold-catalyzed hydration of internal alkynes using mixed P(III)/P(V) cavitands, in which the two phosphorus atoms are *cis*- or *trans*-positioning, *cis*-**3**•AuCl or *trans*-**6**•AuCl, respectively (Scheme 4). For hydration of 1-phenyl-1-butyne, the *cis*-**3**•AuCl led to low activity and selectivity (in part (a)): 1-phenyl-1-butanone (**7d**) and 1-phenyl-2-butanone (**7e**) were obtained in 5 % and 10 % yield, respectively. While repeating the run with *trans*-**6**•AuCl, the compounds **7d** and **7e** were isolated in 2 % and 88 % yield, respectively. A better regioselectivity was also observed when *trans*-**6**•AuCl was employed in the hydration of 3-octyne, the ratio 4-octanone (**7f**)/3-octanone (**7g**) = 9:91 (in part (b)). The ratio **7f**/**7g** decreased to 46:54 when *cis*-**3**•AuCl was used. These results indicate that less anisotropic effect in the *cis*-cavitand would cause less stabilization effect by π-orbital mixing with reaction process, and that the geometrically open space in *cis*-form allows various transition-state geometries to lower selectivity.[18]

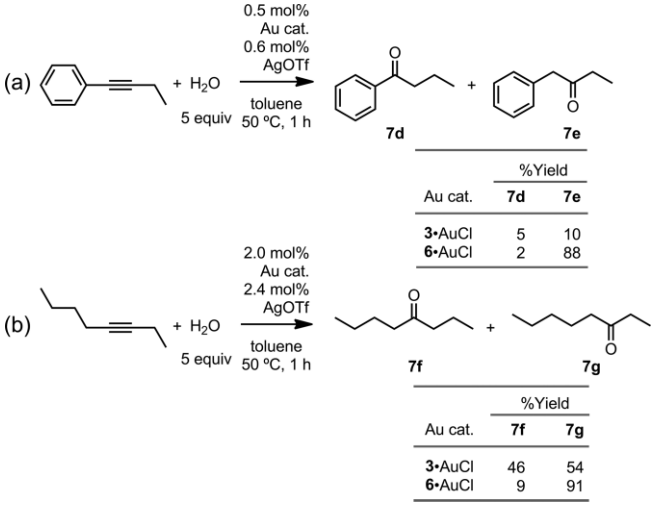

Scheme 4. Catalytic evaluation of *cis*-**3**•AuCl and *trans*-**6**•AuCl in hydration reactions of (a) ethynylbenzene, and (b) 3-octyne.

Next, the three cavitands bearing phosphoramidite moieties (*cis*-**2**, *trans*-**5** and **8**[19]) were assessed in styrene hydroformylation (Figure 3, Scheme 5). The catalytic systems were generated in situ by mixing ligand with $Rh(acac)(CO)_2$ precursor, and the reactions were carried out in toluene under 20 bar of CO/H_2 (1:1) with a styrene/Rh ratio of 5000.

In a first series of tests that are conducted at 80 °C in 24 h, varied amount of the cavitand was studied (Table 1). The numbers of P/Rh ratio were varied from 2 to 10. In the case of mono-dentate **8**, conversions of 64 % and 54 % were measured when P/Rh ratios of 2 and 10 were employed, respectively (entries 7 and 9). Di-phosphoramidites *cis*-**2** and *trans*-**5** were more efficient than **8**, because conversions of 96 %, 99 % and 64 %,

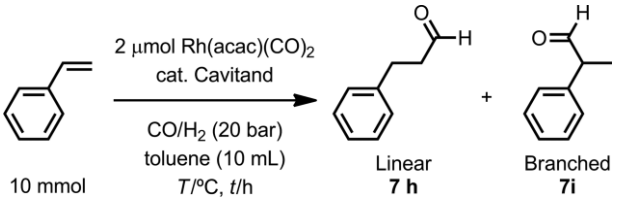

Scheme 5. Rhodium-catalyzed hydroformylation reaction of styrene.

respectively, were observed in a P/Rh ratio of 4 (entries 2, 5 and 8). Interestingly, the product distribution of around **7h**/**7i** = 35:65 was not affected by the excess of *cis*-**2**, contrary to the other two (entries 1–3). Actually, in the case of *trans*-**5**, the P/Rh ratio drastically affects the distribution (entries 4–6): the proportion of branched aldehyde increases with the number of extra-added *trans*-**5**. The distributions were mostly the same when *trans*-**5** or **8** was used in P/Rh = 10, the branched was formed in 78 % or 76 %, respectively (entries 6 and 9).

Table 1. Catalytic evaluation of *cis*-**2**, *trans*-**5**, and **8** in styrene hydroformylation: influence of P/Rh ratios.[a]

Entry	Ligand	P/Rh[b]	Conv./%	Product distribution	
				Linear	Branched
1		2	91	35	65
2	*cis*-**2**	4	96	34	66
3		10	100	37	63
4		2	98	52	48
5	*trans*-**5**	4	99	39	61
6		10	99	22	78
7		2	64	31	69
8	**8**	4	64	31	69
9		10	54	24	76

[a] Reactions were carried out in conditions of Scheme 5 at 80 °C for 24 h. The conversions and products distributions were determined by GC (*n*-decane as internal standard) and by ^1H NMR. [b] Ratios of phosphorus atom per rhodium atom.

In a second series of runs, we investigated the influence of the temperature from 60 °C to 140 °C for 5 h in a P/Rh ratio of 2 (Table 2). As general trends, the conversion increases with the temperature up, and the regioselectivity of the catalysis changes from mainly branched aldehyde at low temperature to mainly linear aldehyde at high temperature. For example, in a use of *trans*-**5**, conversion of 52 % with 16:84 ratio were observed at 60 °C against a full conversion with 64:36 ratio at 120 °C (entries 8 and 13). For the tests carried out at 140 °C, lower conversions arose from catalyst decomposition (entries 7 and 21). We observed di-phosphane (*cis*-**2** and *trans*-**5**) led to higher activities than mono-phosphane **8**, especially at low temperature. In fact, at 60 °C, conversions of 59 %, 52 % and 11 % were measured when ligands *cis*-**2**, *trans*-**5** and **8** were employed, respectively (entries 1, 8 and 15). Similarly, a higher distribution toward linear aldehyde was observed when *cis*-**2** and *trans*-**5** were used rather than **8**, proportion of 35 %, 51 % and 31 % were obtained, respectively (entries 2, 9 and 16). Once the rhodium complexes formed in situ, the catalysts kept the stable state, because similar catalytic outcomes were observed during the first 5 h of reactions at 120 °C (entries 4–6, 11–13 and 18–20). The main differences between *cis*-**2** and *trans*-**5** is

that *cis*-**2** produced less thermally stable active species than those formed by *trans*-**5**, because lower activities were measured at 120 °C and 140 °C (entries 5–7 and 12–14). Actually, at the end of the reaction course in use of *cis*-**2**, small amounts of black insoluble materials, presumably rhodium colloids were observed.

Table 2. Catalytic evaluation of *cis*-**2**, *trans*-**5**, and **8** in styrene hydroformylation: influence of the temperature.[a]

Entry	Ligand	*T*/°C	*t*/h	Conv./%	Product distribution	
					Linear/%	Branched/%
1	*cis*-**2**	60	5	59	33	67
2		80	5	88	35	65
3		100	5	92	56	43
4		120	0.5	41	66	34
5		120	2	48	63	37
6		120	5	69	65	35
7		140	5	60	62	38
8	*trans*-**5**	60	5	52	16	84
9		80	5	75	51	49
10		100	5	89	58	42
11		120	0.5	48	56	44
12		120	2	89	63	37
13		120	5	100	64	36
14		140	5	100	64	36
15	**8**	60	5	11	18	82
16		80	5	40	31	68
17		100	5	82	58	42
18		120	0.5	17	56	44
19		120	2	69	66	34
20		120	5	91	64	36
21		140	5	54	68	32

[a] Reactions were carried out in conditions of Scheme 5 with P/Rh = 2 (ratio of phosphorus atom per rhodium atom). The conversion and product distributions were determined by GC (*n*-decane as internal standard) and by ^{1}H NMR.

From these hydroformylations, the following information of the catalyst systems could be deduced: for **8**, due to the steric hindrance, formation of RhL_2 complex should be excluded. Generation of singly ligated active species favor the formation of Rh(η^3-styrenyl)(**8**)$(CO)_2$ over the less stable Rh(σ-ethylphenyl)(**8**)$(CO)_2$ species; which means the catalyst favors formation of the branched aldehyde at low temperature.[20] At high temperature, thermal agitation generates strong steric interactions between the coordinated substrate and cavity wall; such metal confinement favors the formation of the linear aldehyde.[21] For *trans*-**5**, due to the distance between the two phosphorus atoms (9.7 Å based on the crystallographic result of *trans*-**5**·$(AuCl)_2$),[8] formation of rhodium-chelate complexes should be excluded. Nevertheless, the proximity of two-coordinated rhodium atoms, on the same cavitand, may allow to consider a cooperation between these two metal centers.[22] In fact, the higher activity and selectivity toward the linear aldehyde regarding **8** are arguments in that sense. Furthermore, when a large excess of *trans*-**5** was used, we can assume that only one atom of rhodium is coordinated to the ligand and the second phosphorus atom remained free: actually, product distributions in *trans*-**5** and **8** were mostly the same. For *cis*-**2**, according to molecular modeling, the distance between the two phosphorus atoms (ca. 6.5 Å) was important to allow the formation of rhodium-chelate complexes. The shorter distance, compared to *trans*-**5**, should reinforce the cooperation between the two metal centers, which led to a more efficient system as observed at low temperature. However, the shorter distance may be responsible for the low thermal stability and rhodium agglomeration. The *cis*-**2** has wider open cavity than *trans*-**5**, so the steric hindrance generated by the two quinoxaline-walls was reduced; consequently, the proportion of branched aldehyde might increase. Moreover, in the case of *cis*-**2**, according to molecular modeling, the distance between the two phosphorus atoms (ca. 6.5 Å) exclude the formation of rhodium-chelate complexes. The shorter distance, compared to *trans*-**5**, should reinforce the cooperation between the two metal centers, which led, as observed at low temperature, to a more efficient catalytic system. However, the shorter distance between the two rhodium atoms and the more open structure may be responsible at high temperature for the lower stability for the active species. Their degradation led to the formation of rhodium-rhodium bonds and *in fine* to the formation of colloids.

Conclusions

In summary, three cavitands having a *cis*-arrangement of two quinoxaline walls (*cis*-**1**, –**2**, and –**3**) were successfully synthesized. These cavitands, in which two catalytic centers are inwardly oriented, provide new architecture for transition metal catalysis. Gold-catalyzed dimerization and hydration of alkynes and rhodium-catalyzed styrene hydroformylation were carried out with these *cis*-type cavitands. Comparative studies with isomers *trans*-**4**, –**5**, and –**6** allow us to evaluate the structure-activity relationship. The catalytic results strongly suggest two salient features. Firstly, the less impeded *cis*-environment around the metal center reduced or modified the product distribution as compared to those observed with *trans*-spanned ligand. Secondly, the distance between the two phosphorus atoms is shorter in the *cis*-types than *trans*-versions: although a shorter distance promotes cooperation between the two metal centers, as observed in the styrene hydroformylation, it might favor the leach of the rhodium metal away from the ligand and formation of rhodium aggregations. To the best of our knowledge, this work represents the first examples in homogeneous catalysis of comparative studies involving ligands built on extended cavitands having a *cis*- or a *trans*-positioning of two active centers. Further developments of cavitand catalysts are ongoing and will be reported in due course.

Experimental Section

General Methods: All reactions sensitive to air or moisture were carried out under an argon or a nitrogen atmosphere and anhydrous conditions unless otherwise noted. Dry solvents were purchased and used without further purification and dehydration. All

reagents were purchased and used without further purification. Analytical thin layer chromatography was carried out on Merck silica $60F_{254}$. Column chromatography was carried out with silica gel 60_N (Kanto Chemical Co.). LRMS and HRMS were reported on the basis of TOF (time of flight)-MS (MADI-TOF or LCMS-IT-TOF), and DART (Direct Analysis in Real Time)-MS. ^1H and ^{13}C NMR spectra were recorded with a 5 mm QNP probe at 400 MHz and 100 MHz, respectively. Chemical shifts are reported in d (ppm) with reference to residual solvent signals [^1H NMR: $CHCl_3$ (7.26), C_7H_8 (2.08), C_6H_6 (7.16), CH_2Cl_2 (5.32); ^{13}C NMR: $CDCl_3$ (77.0)]. Signal patterns are indicated as s, singlet; d, doublet; t, triplet; q, quartet; m, multiplet; br, broad. Assignment of ^{13}C NMR was carefully performed with labeling the corresponding numbers those were listed in ^{13}C NMR spectra.

Synthesis of 1 and *iso*-1: (see Scheme 1 (a) and (b)) To the Schlenk tube charged with a solution of the tetra-hydroxy *cis*-cavitand (407 mg, 0.3 mmol) in dry toluene (3 mL) under N_2 at 135 °C, $EtN(iPr)_2$ (0.52 mL, 3.0 mmol) and $P(OCH_3)_3$ (0.29 mL, 2.4 mmol) were added. After stirred for 6 h, the reaction mixture was cooled to room temperature and concentrated to give 457 mg of crude products as pale yellow solid materials. Purification by silica-gel column chromatography (eluent: hexane/EtOAc, 19:1) afforded 195 mg of **1** ("out-out") as white solid materials in 44 % yield and 98 mg of *iso*-**1** ("in-out") as white solid materials in 22 % yield.

Data for **1**: ^1H NMR (400 MHz, $CDCl_3$) 8.41 (s, 1H), 7.98 (d, J = 8.2 Hz, 2H), 7.82 (d, J = 8.2 Hz, 2H), 7.62–7.52 (m, 4H), 7.38 (s, 2H), 7.21 (s, 3H), 7.17 (s, 1H), 6.46 (s, 1H), 5.73 (t, J = 7.8 Hz, 2H), 4.54 (t, J = 7.8 Hz, 2H), 3.88 (d, $^3J_{PH}$ = 8.6 Hz, 6H, $POCH_3$), 2.30–2.17 (m, 8H), 1.43–1.27 (m, 72H), 0.90–0.87 (m, 12H) ppm; ^1H NMR (400 MHz, [D_8]toluene) 8.82 (s, 1H), 7.85 (d, J = 8.2 Hz, 2H), 7.78 (s, 2H), 7.69 (s, 2H), 7.66 (s, 2H), 7.58 (s, 1H), 7.49 (d, J = 8.2 Hz, 2H), 7.18 (dd, J = 8.1, 7.4 Hz, 2H), 7.06–7.01 (m, 2H), 6.32 (s, 1H), 6.14 (t, J = 8.1 Hz, 2H), 4.87 (t, J = 7.8 Hz, 2H), 3.65 (d, $^3J_{PH}$ = 8.6 Hz, 6H, $POCH_3$), 2.46–2.35 (m, 8H), 1.50–1.29 (m, 72H), 0.97–0.92 (m, 12H) ppm; $^{13}C\{^1H\}$ NMR (100 MHz, $CDCl_3$) 153.2, 153.03, 152.98, 152.9, 147.3, 147.2, 147.10, 147.06, 140.03, 137.6 (d, $J_{C,P}$ = 2.6 Hz), 136.5, 135.3, 129.6, 129.4, 128.4, 128.2, 123.8, 122.9, 122.3, 119.2, 118.1, 117.4, 50.4 (d, $J_{C,P}$ = 2.6 Hz), 35.9, 34.4, 32.9, 32.3 (many peaks are overlapped), 30.1 (many peaks are overlapped), 29.8 (many peaks are overlapped), 28.4, 28.3, 23.1 (many peaks are overlapped), 14.5 (many peaks are overlapped) ppm; $^{31}P\{^1H\}$ NMR (162 MHz, $CDCl_3$) 127.3 ppm; MS (ESI) *m/z*: 1512 [M + Cl]$^-$; IR (neat): $\tilde{\nu}$ = 2922, 2851, 1606, 1578, 1482, 1412, 1332, 1158, 1029, 759 cm^{-1}; HRMS (ESI) calcd. for $C_{90}H_{118}N_4O_{10}P_2Cl$: 1511.8017 [M + Cl]$^-$, found 1511.8000.

Data for *iso*-**1**: ^1H NMR (400 MHz, $CDCl_3$) 8.36 (s, 1H), 7.99 (d, J = 8.0 Hz, 1H), 7.97 (d, J = 7.8 Hz, 1H), 7.84 (d, J = 8.1 Hz, 1H), 7.644 (d, J = 8.2 Hz, 1H), 7.643–7.51 (m, 4H), 7.39 (s, 1H), 7.28 (s, 1H), 7.22 (s, 2H), 7.15 (s, 1H), 7.11 (s, 1H), 6.31 (s, 1H), 5.76 (t, J = 7.8 Hz, 1H), 5.71 (t, J = 7.8 Hz, 1H), 4.53–4.46 (m, 2H), 3.87 (d, $^3J_{PH}$ = 8.6 Hz, 3H, $POCH_3$), 3.21 (d, $^3J_{PH}$ = 12.6 Hz, 3H, $POCH_3$), 2.29–2.17 (m, 8H), 1.41–1.27 (m, 72H), 0.90–0.87 (m, 12H) ppm; ^1H NMR (400 MHz, [D_8]toluene) 8.82 (s, 1H), 8.03 (d, J = 8.3 Hz, 1H), 7.81 (d, J = 8.3 Hz, 1H), 7.69 (s, 1H), 7.66 (s, 1H), 7.63 (s, 1H), 7.56 (s, 2H), 7.50 (s, 1H), 7.42 (d, J = 8.2 Hz, 1H), 7.39 (d, J = 8.2 Hz, 1H), 7.26 (dd, J = 8.2, 7.3 Hz, 1H), 7.18 (dd, J = 8.2, 7.3 Hz, 1H), 7.05–7.01 (m, 2H), 6.38 (s, 1H), 6.15 (t, J = 8.1 Hz, 1H), 6.08 (t, J = 8.1 Hz, 1H), 4.91 (t, J = 7.9 Hz, 1H), 4.75 (t, J = 7.9 Hz, 1H), 3.72 (d, $^3J_{PH}$ = 8.6 Hz, 3H, $POCH_3$), 2.43–2.32 (m, 8H), 2.04 (d, $^3J_{PH}$ = 12.4 Hz, 3H, $POCH_3$), 1.48–1.29 (m, 72H), 0.95–0.93 (m, 12H) ppm; $^{13}C\{^1H\}$ NMR (100 MHz, $CDCl_3$) 153.3, 153.23, 153.19, 153.1, 153.0, 152.9, 152.7, 152.4 (d, $J_{C,P}$ = 1.2 Hz), 148.8, 148.6 (d, $J_{C,P}$ = 6.2 Hz), 148.5, 147.3 (d, $J_{C,P}$ = 4.5 Hz), 146.6 (d, $J_{C,P}$ = 2.4 Hz), 140.34, 140.31, 140.28, 140.2, 137.8 (d, $J_{C,P}$ = 2.6 Hz), 136.54, 136.45, 135.9, 135.7, 135.4, 134.8, 134.4, 129.8, 129.7, 129.5, 129.4, 128.5, 128.3, 127.8, 124.1, 123.1, 122.6, 121.7, 119.1, 118.0, 117.7, 116.8, 51.9 (d, $J_{C,P}$ = 22.2 Hz), 50.2 (d, $J_{C,P}$ = 2.6 Hz), 36.7, 35.9, 34.5, 34.4, 32.8, 32.5, 32.3 (many peaks are overlapped), 31.8, 31.1, 30.2, 30.12, 30.09 (many peaks are overlapped), 30.05, 30.01, 29.78, 29.75, 28.4, 28.3, 23.1, 23.0 (many peaks are overlapped), 14.5 (many peaks are overlapped) ppm; $^{31}P\{^1H\}$ NMR (162 MHz, $CDCl_3$) 125.6, 110.6 ppm; MS (ESI) *m/z*: 1512 [M + Cl]$^-$; IR (neat): $\tilde{\nu}$ = 2922, 2851, 1578, 1482, 1412, 1352, 1146, 1029, 760 cm^{-1}; HRMS (ESI) calcd. for $C_{90}H_{118}N_4O_{10}P_2Cl$: 1511.8021 [M + Cl]$^-$, found 1511.8021.

Synthesis of 2: (see Scheme 1 (a)) To the tetra-hydroxy *cis*-cavitand platform (272 mg, 0.2 mmol) in a 20 mL Schlenk tube under Ar were added toluene (2 mL) and Et_3N (0.13 mL, 0.96 mmol). After the mixture was stirred for 10 min, $P[N(CH_3)_2]_3$ was added and the reaction mixture was heated at 75 °C for 1 h. The mixture was cooled to room temperature, filtered, washed with toluene, and then the filtrate was concentrated in vacuo to give 309 mg of crude products. Purification by short-plugged column chromatography (eluent, $CHCl_3$ only) afforded 138 mg of white solid materials, which were recrystallized from EtOH/EtOAc (8 mL/4.5 mL) to yield **2** in 40 % (120 mg) as colorless crystals. ^1H NMR (400 MHz, $CDCl_3$) 8.39 (s, 1H), 7.99 (dd, J = 8.5, 8.4 Hz, 2H), 7.80 (dd, J = 8.2, 1.4 Hz, 2H), 7.61–7.51 (m, 4H), 7.32 (s, 2H), 7.19 (s, 1H), 7.18 (s, 2H), 7.12 (s, 1H), 6.33 (s, 1H), 5.70 (t, J = 8.2 Hz, 2H), 4.55 (t, J = 7.6 Hz, 2H), 2.77 (d, $^3J_{PH}$ = 10.6 Hz, 12H, $N(CH_3)_2$), 2.28–2.17 (m, 8H), 1.41–1.27 (m, 72H), 0.90–0.87 (m, 12H) ppm; ^1H NMR (400 MHz, [D_8]toluene) 8.83 (s, 1H), 7.88 (d, J = 8.2 Hz, 2H), 7.75 (s, 2H), 7.72 (s, 1H), 7.68 (s, 2H), 7.60 (s, 1H), 7.48 (d, J = 8.2 Hz, 2H), 7.19 (ddd, J = 8.2, 8.2, 1.0 Hz, 2H), 7.05–7.01 (m, 2H), 6.15 (t, J = 8.1 Hz, 2H), 4.97 (t, J = 7.4 Hz, 2H), 2.52 (d, $^3J_{PH}$ = 10.2 Hz, 12H, $N(CH_3)_2$), 2.49–2.09 (m, 8H), 1.51–1.30 (m, 72H), 0.96–0.93 (m, 12H) ppm; $^{13}C\{^1H\}$ NMR (100 MHz, $CDCl_3$) 153.3, 153.1, 153.0, 152.6, 149.8 (two peaks are overlapped), 149.3 (two peaks are overlapped), 140.3 (d, $^4J_{CP}$ = 9.3 Hz), 137.7, 136.5, 135.7, 134.5, 129.2, 128.3, 123.9, 122.6, 121.8, 119.1, 117.8, 117.0, 35.4 (d, $^2J_{CP}$ = 18.8 Hz, two peaks are overlapped), 35.8, 34.4, 32.6, 32.3, 31.6, 30.1, 29.8, 28.4, 28.3, 23.1, 14.5 (many peaks are overlapped) ppm; $^{31}P\{^1H\}$ NMR (162 MHz, $CDCl_3$) 140.6 ppm; MS (ESI) *m/z*: 1539 [M + Cl]$^-$; IR (neat): $\tilde{\nu}$ = 2922, 2851, 1577, 1481, 1412, 1332, 1158, 977, 758 cm^{-1}; HRMS (ESI) calcd. for $C_{92}H_{124}N_6O_8P_2Cl$: 1538.8678, found 1538.8668; Anal. Calcd for $C_{92}H_{124}N_6O_8P_2$: C, 73.47; H, 8.31; N, 5.59; found C, 73.47; H, 8.37; N, 5.66.

Synthesis of 3: (see Scheme 1(c)) To **1** (148 mg, 0.1 mmol) in toluene (4 mL) at 0 °C was slowly added a cooled-toluene solution of mCPBA (75 %, 23 mg, 0.1 mmol) over 3 min. After stirring at 0 °C for 1.5 h, the reaction was quenched with saturated aqueous $NaHCO_3$ (2 mL), and stirred at ambient temperature for 30 min. The mixture was transferred into a 50 mL separatory funnel, washed with water (10 mL) and brine (10 mL), dried with Na_2SO_4, and concentrated in vacuo to give a crude of 143 mg as a white solid material. Purification by short-plugged column chromatography (SiO_2, toluene/EtOAc = 9:1) led to 44 mg of **3** in 30 % yield as white solid powder. ^1H NMR (400 MHz, $CDCl_3$) 8.43 (s, 1H), 8.13 (d, J = 8.3 Hz, 1H), 7.87 (d, J = 8.5 Hz, 1H), 7.84–7.82 (m, 1H), 7.79–7.77 (m, 1H), 7.70 (dd, J = 8.1, 7.0 Hz, 1H), 7.59 (dd, J = 7.6, 7.3 Hz, 1H), 7.49–7.46 (m, 2H), 7.44 (s, 1H), 7.42 (s, 1H), 7.23 (s, 1H), 7.17 (s, 3H), 6.58 (s, 1H), 5.79–5.71 (m, 2H), 4.61 (t, J = 7.6 Hz, 1H), 4.49 (t, J = 7.6 Hz, 1H), 4.00 (d, $^3J_{PH}$ = 11.3 Hz, 3H), 3.88 (d, $^3J_{PH}$ = 8.9 Hz, 3H), 2.36–2.24 (m, 8H), 1.41–1.28 (m, 72H), 0.92–0.87 (m, 12H) ppm; ^1H NMR (400 MHz, [D_8]toluene) 8.82 (s, 1H), 7.98 (d, J = 8.2 Hz, 1H), 7.95 (s, 1H), 7.77 (s, 1H), 7.69–7.59 (m, 5H), 7.49 (s, 1H), 7.48 (d, J = 8.2 Hz, 1H), 7.26 (m, 2H), 7.16–6.93 (m, 2H), 7.61 (s, 1H), 6.20 (t, J = 8.0 Hz,

1H), 6.11 (t, *J* = 8.0 Hz, 1H), 4.90 (t, *J* = 7.6 Hz, 1H), 4.77 (t, *J* = 7.6 Hz, 1H), 3.55 (d, $^3J_{PH}$ = 11.3 Hz, 3H), 3.45 (d, $^3J_{PH}$ = 8.9 Hz, 3H), 2.47–2.29 (m, 8H), 1.33–1.28 (m, 72H), 0.96–0.92 (m, 12H) ppm; $^{13}C\{^1H\}$ NMR (100 MHz, $CDCl_3$) 153.5, 153.3, 153.0, 152.8, 152.7, 147.6, 147.2 (d, $J_{C,P}$ = 3.8 Hz), 146.34, 146.28, 146.1 (d, $J_{C,P}$ = 6.91 Hz), 140.41, 140.38, 140.31, 140.27, 138.0, 137.2, 136.9 (d, $J_{C,P}$ = 1.9 Hz), 136.6, 135.8, 135.3, 134.4 (d, $J_{C,P}$ = 4.5 Hz), 133.0, 132.9, 129.7, 129.6, 129.4, 129.2, 128.7, 128.4, 128.24, 128.20, 123.6, 123.0, 122.5, 122.3, 119.3, 118.8, 117.03, 116.99, 116.93, 56.0 (d, $J_{C,P}$ = 6.2 Hz), 50.2, 36.0, 35.9, 34.5, 34.4, 33.1, 32.3, 32.1, 31.5, 31.4, 30.1 (many peaks are overlapped), 29.8 (many peaks are overlapped), 28.4, 28.3, 23.1 (many peaks are overlapped), 14.5 (many peaks are overlapped) ppm; $^{31}P\{^1H\}$ NMR (162 MHz, $CDCl_3$) 125.7, –13.6 ppm; MS (ESI) *m/z*: 1528 $[M + Cl]^-$; IR (neat): $\tilde{\nu}$ = 2922, 2851, 1578, 1482, 1412, 1352, 1146, 1029, 760 cm^{-1}; HRMS (ESI) calcd. for $C_{90}H_{118}N_4O_{11}P_2Cl$: 1527.7966 $[M + Cl]^-$, found 1527.7967.

Synthesis of 1·(AuCl)$_2$ and 3·AuCl: (see Scheme 2) For **1**·(AuCl)$_2$: Under N_2 atmosphere, a solution of **1** (148 mg, 0.1 mmol) in toluene (2 mL) underwent addition of AuCl·S(CH$_3$)$_2$ (71 mg, 0.24 mmol), and the mixture was stirred for 40 min, consumption of **1** was monitoring by TLC. After all the volatiles had been evaporated, 174 mg of as white powder materials, corresponding to **1**·(AuCl)$_2$ complex was isolated in quantitative yield. ^1H NMR (400 MHz, $CDCl_3$) 8.33 (s, 1H), 7.92–7.90 (m, 4H), 7.64–7.58 (m, 4H), 7.46 (s, 2H), 7.31 (s, 1H), 7.29 (s, 2H), 7.24 (s, 1H), 6.82 (s, 1H), 5.77 (t, *J* = 8.0 Hz, 2H), 4.44 (t, *J* = 7.3 Hz, 2H), 4.02 (d, $^3J_{P,H}$ = 13.8 Hz, 6H), 2.30–2.17 (m, 8H), 1.45–1.27 (m, 72H), 0.90–0.87 (m, 12H) ppm; $^{13}C\{^1H\}$ NMR (100 MHz, $CDCl_3$) 153.2 (d, $J_{C,P}$ = 1.7 Hz), 153.1 (two peaks are overlapped), 152.2, 152.0, 145.3, 144.6, 140.2, 140.1 (two peaks are overlapped), 137.9 (d, $J_{C,P}$ = 1.9 Hz), 137.0, 136.0, 135.7, 130.2, 130.0, 129.6, 127.5, 123.4, 123.2, 119.0, 118.3, 55.1 (POCH$_3$), 36.0, 34.4, 32.2 (many peaks are overlapped), 31.2, 30.0 (many peaks are overlapped), 29.9 (many peaks are overlapped), 29.9, (many peaks are overlapped), 29.8, 29.7 (many peaks are overlapped), 28.2, 28.1, 23.0, 22.9, 14.4 ppm; $^{31}P\{^1H\}$ NMR (162 MHz, $CDCl_3$) 99.4 ppm; MS (ESI) *m/z*: 1906 $[M - Cl]^+$; IR (neat): $\tilde{\nu}$ = 2925, 2857, 1483, 1408, 1328, 1148, 1029, 905, 759, 599 cm^{-1}; HRMS (ESI) calcd. for $C_{90}H_{118}Au_2ClN_4O_{10}P_2$: 1905.7343 $[M - Cl]^+$, found 1905.7394.

For **3**·AuCl: Under N_2 atmosphere, a solution of **3** (111 mg, 0.074 mmol) in toluene (1.2 mL) underwent addition of AuCl·S(CH$_3$)$_2$ (26 mg, 0.089 mmol), and the reaction mixture was stirred for 30 min, consumption of **3** was monitoring by TLC. After all the volatiles had been evaporated, the crude products were purified by short-plugged silica-gel column chromatography (eluent: hexane/EtOAc, 1:1) to afford 56 mg of **3**·AuCl as white powder materials in 63 % yield. ^1H NMR (400 MHz, $CDCl_3$) 8.40 (s, 1H), 8.11 (d, *J* = 8.4 Hz, 1H), 7.95 (d, *J* = 8.4 Hz, 1H), 7.88 (d, *J* = 8.4 Hz, 1H), 7.78 (d, *J* = 8.4 Hz, 1H), 7.72 (dd, *J* = 8.4, 8.4 Hz, 1H), 7.63 (dd, *J* = 8.4, 8.4 Hz, 1H), 7.56 (s, 1H), 7.53–7.46 (m, 2H), 7.39 (s, 1H), 7.21 (s, 1H), 7.20 (s, 1H), 7.19 (s, 1H), 7.15 (s, 1H), 6.73 (s, 1H), 5.81 (t, *J* = 8.0 Hz, 1H), 5.77 (t, *J* = 8.3 Hz, 1H), 4.51 (t, *J* = 8.1 Hz, 1H), 4.50 (t, *J* = 8.2 Hz, 1H), 4.07 (d, $^3J_{P,H}$ = 13.9 Hz, 3H), 3.99 (d, $^3J_{P,H}$ = 11.4 Hz, 3H), 2.36–2.21 (m, 8H), 1.48–1.27 (m, 72H), 0.90–0.87 (m, 12H) ppm; $^{13}C\{^1H\}$ NMR (100 MHz, $CDCl_3$) 153.6 (two peaks are overlapped), 153.1, 152.8 (two peaks are overlapped), 152.7, 152.5, 152.0, 146.8 (d, $J_{C,P}$ = 6.4 Hz), 146.3 (d, $J_{C,P}$ = 6.4 Hz), 144.3 (d, $J_{C,P}$ = 5.5 Hz), 143.8 (d, $J_{C,P}$ = 4.8 Hz), 140.44, 140.36, 140.3, 140.2, 138.0 (d, $J_{C,P}$ = 1.7 Hz), 137.1 (d, $J_{C,P}$ = 4.8 Hz), 136.1, 135.9, 135.8, 135.5, 135.4, 133.6 (d, $J_{C,P}$ = 3.6 Hz), 130.0, 129.9, 129.8, 129.7, 129.3, 128.8, 128.1, 127.8, 123.7, 123.0, 122.8, 122.5, 119.2, 118.4 (d, $J_{C,P}$ = 3.8 Hz), 117.0 (d, $J_{C,P}$ = 4.3 Hz), 116.5, 56.0 (d, $^2J_{C,P}$ = 6.0 Hz), 54.7 (d, $^2J_{C,P}$ = 2.9 Hz), 36.0, 34.4, 33.2, 32.3 (many peaks are overlapped), 31.8, 30.4, 30.1 (many peaks are overlapped), 30.0 (many peaks are overlapped), 29.8, 29.7, 23.0 (many peaks are overlapped), 14.5 (many peaks are overlapped) ppm; $^{31}P\{^1H\}$ NMR (162 MHz, $CDCl_3$) 112.8, –7.60 ppm; MS (ESI) *m/z*: 1760 $[M + Cl]^-$; IR (neat): $\tilde{\nu}$ = 2921, 2849, 1483, 1408, 1328, 1145, 1041, 914, 759 cm^{-1}; HRMS (ESI) calcd. for $C_{90}H_{118}AuCl_2N_4O_{11}P_2$: 1759.7320 $[M + Cl]^-$, found 1759.7350.

Representative procedure for Au-catalyzed dimerization of terminal alkynes: (see Scheme 3) Under N_2 atmosphere, the bis-Au catalyst (0.01 mmol) in a 25 mL two-necked flask was dissolved in toluene (5 mL; containing traces of water), and the starting alkynes of ethynylbenzene (102 mg, 1 mmol) and the other partner 1-octyne (165 mg, 1.5 mmol) were added. After addition of AgOTf (5.0 mg, 0.02 mmol) at room temperature, the reaction was conducted for 20 h. The solvent was evaporated off, and filtered through a short-plugged column chromatography to give a crude product. The crude materials consisted of just starting alkynes and/or product **7a**, **7b**, and **7c** because of clean reaction progress: thus, chemical yields and molar ratios of products were determined in the crude state. All dimer adducts were identical to the authentic samples that we previously reported.[10]

Representative procedure for Au-catalyzed hydration of internal alkynes: (see Scheme 4) Complex **1**·(AuCl)$_2$ (17 mg, 0.01 mmol) was added under Ar to a solution of 3-octyne (0.07 mL, 0.5 mmol) in [D_8]toluene (1 mL) and H_2O (0.05 mL, 2.5 mmol). The mixture was stirred at room temperature for 5 min, AgOTf (3 mg, 0.012 mmol) was then added, and the whole system was immersed in a 50 °C preheated oil bath. After stirred for 1 h, the reaction mixture was cooled to ambient temperature. Purification by short-plug silica-gel column chromatography with use of a Pasteur pipette and [D_8]toluene as eluent gave a colorless C_7D_8 solution. ^1H NMR spectroscopy determined the chemical yields and product distribution (proportions of **7f** and **7g**).[11] ^1H NMR spectroscopic data for **7f** and **7g** were identical to those for commercially available authentic sample.

Representative procedure for Rh-catalyzed hydroformylation of styrene: (see Scheme 5) The hydroformylation reactions were carried out in a glass-lined, 50 mL stainless steel autoclave containing a magnetic stirring bar, then the autoclave was closed and flushed twice with vacuum/N_2. To the vessel were added toluene (8 mL), styrene (10 mmol), *n*-decane (0.5 mL), 1 mL toluene solution of Rh(acac)(CO)$_2$ (2 μmol), and 1 mL toluene solution of appropriate ligand. After pressurized at 20 bar (CO/H_2 1:1) and heated at appropriate temperature for the adequate time, the autoclave was cooled to ambient temperature before being depressurized. The reaction mixture was analyzed by GC using a WCOT fused-silica gel column chromatography (25 m × 0.25 mm) and by ^1H NMR.

Supporting Information (see footnote on the first page of this article): ^1H NMR and ^{13}C NMR and ^{31}P NMR spectra for all new compounds of *cis*-**1**, *cis*-**2**, *cis*-**3**, **1**·(AuCl)$_2$ and **3**·AuCl.

Acknowledgments

JSPS Grant-in-Aid for Scientific Research (C), Grant Number 19K05426, which supported T. I. in this work, is gratefully acknowledged for generous funding. The authors thank Dr. Toshiyuki Iwai and Dr. Takatoshi Ito at ORIST for gentle assistance with HRMS. Prof. Dr. Schramm, M. P. at CSULB are gratefully thanked for helpful discussions. S. H. gratefully acknowledges the University of Carthage and the Tunisian Ministère de l'Enseignement Supérieur et de la Recherche Scientifique for financial support.

Keywords: Introverted ligands · Cavitands · Structure-activity relationships · Homogeneous catalysis

[1] a) R. Breslow, *Acc. Chem. Res.* **1995**, *28*, 146–153; b) P. D. Frischmann, M. J. MacLachlan, *Chem. Soc. Rev.* **2013**, *42*, 871–890, and references cited therein; c) P. Ballester, M. Fujita, J. Rebek Jr., *Chem. Soc. Rev.* **2015**, *44*, 392–393 and references cited therein.

[2] a) R. J. Hooley, J. Rebek Jr., *Chem. Biol.* **2009**, *16*, 255–264, and references cited therein; b) A. Galan, P. Ballester, *Chem. Soc. Rev.* **2016**, *45*, 1720–1737; c) D. M. Kaphan, F. D. Toste, R. G. Bergman, K. N. Raymond, *J. Am. Chem. Soc.* **2015**, *137*, 9202–9205; d) M. Guitet, P. Zhang, F. Marcelo, C. Tugny, J. Jimnez-Barbero, O. Buriez, C. Amatore, V. Mouris-Mansuy, J.-P. Goddard, L. Fensterbank, Y. Zhang, S. Roland, M. Mnand, M. Sollogoub, *Angew. Chem. Int. Ed.* **2013**, *52*, 7213–7218; *Angew. Chem.* **2013**, *125*, 7354.

[3] a) B. Cornils, W. A. Herrmann, *Applied Homogeneous Catalysis with Organometallic Compounds*, Wiley-VCH, Weinheim, Germany, 2nd Ed. **2002**; b) R. A. Sheldon, I. Arends, U. Hanefeld, *Green Chemistry and Catalysis*, Wiley-VCH, Weinheim, Germany, **2007**.

[4] a) J. R. Moran, S. Karbach, D. J. Cram, *J. Am. Chem. Soc.* **1982**, *104*, 5826–5828; b) A. R. Renslo, J. Rebek Jr., *Angew. Chem. Int. Ed.* **2000**, *39*, 3281–3283; *Angew. Chem.* **2000**, *112*, 3419; c) T. Chavagnan, D. Sémeril, D. Matt, L. Toupet, *Eur. J. Org. Chem.* **2017**, 313–323.

[5] a) Mini-reviews, A. C. H. Jans, X. Caumes, J. N. H. Reek, *ChemCatChem* **2019**, *11*, 287–297; b) Digest review: T. Iwasawa, *Tetrahedron Lett.* **2017**, *58*, 4217–4228; c) N. Natarajan, E. Brenner, D. Sémeril, D. Matt, J. Harrowfield, *Eur. J. Org. Chem.* **2017**, *2017*, 6100–6113.

[6] From the viewpoint of supramolecular catalysis through encapsulation effects, the following papers are relevant reviews, see a) T. S. Koblenz, J. Wassenaar, J. N. H. Reek, *Chem. Soc. Rev.* **2008**, *37*, 247–262; b) M. Yoshizawa, J. K. Klosterman, M. Fujita, *Angew. Chem. Int. Ed.* **2009**, *48*, 3418–3438; *Angew. Chem.* **2009**, *121*, 3470; c) M. J. Wiester, P. A. Ulmann, C. A. Mirkin, *Angew. Chem. Int. Ed.* **2011**, *50*, 114–137; *Angew. Chem.* **2011**, *123*, 118; d) T. R. Cook, V. Vajpayee, M. H. Lee, P. J. Stang, K. W. Chi, *Acc. Chem. Res.* **2013**, *46*, 2464–2474; e) M. Raynal, P. Ballester, A. Vidal-Ferran, P. W. N. M. van Leeuwen, *Chem. Soc. Rev.* **2014**, *43*, 1734–1787; f) S. H. A. M. Leenders, R. Gramage-Doria, B. de Bruin, J. N. H. Reek, *Chem. Soc. Rev.* **2015**, *44*, 433–448; g) C. J. Brown, F. D. Toste, R. G. Bergman, K. N. Raymond, *Chem. Rev.* **2015**, *115*, 3012–3035; h) D. Zhang, A. Martinez, J.-P. Dutasta, *Chem. Rev.* **2017**, *117*, 4900–4942.

[7] F. Diederich, *Angew. Chem. Int. Ed.* **2007**, *46*, 68–69; *Angew. Chem.* **2007**, *119*, 68.

[8] F. Wöhler, *Ann. Chim. Phys.* **1828**, *37*, 330.

[9] a) T. Iwasawa, Y. Nishimoto, K. Hama, T. Kamei, M. Nishiuchi, Y. Kawamura, *Tetrahedron Lett.* **2008**, *49*, 4758–4762; b) M. Kanaura, N. Endo, M. P. Schramm, T. Iwasawa, *Eur. J. Org. Chem.* **2016**, 4970–4975.

[10] N. Endo, M. Kanaura, M. P. Schramm, T. Iwasawa, *Eur. J. Org. Chem.* **2016**, *2016*, 2514–2521.

[11] N. Endo, M. Inoue, T. Iwasawa, *Eur. J. Org. Chem.* **2018**, *2018*, 1136–1140.

[12] P. P. Castro, G. Zhao, G. A. Masangkay, C. Hernandez, L. M. Gutierrez-Tunstad, *Org. Lett.* **2004**, *6*, 333–336.

[13] No resonances of the "in-in" isomer was observed in the ^{1}H NMR spectrum of the crude reaction mixture.

[14] The oxidation with mCPBA led to 24 % of di-phosphate derivative and 46 % of unreacted **1** was recovered.

[15] In compound **5**, crystallographic analysis revealed that, for steric reason, the two $PN(CH_3)_2$ moieties point outside from the cavity, see ref.[8].

[16] V. A. Azov, B. Jaun, F. Diederich, *Helv. Chim. Acta* **2004**, *87*, 449–462.

[17] M. Inoue, K. Ugawa, T. Maruyama, T. Iwasawa, *Eur. J. Org. Chem.* **2018**, *2018*, 5304–5311.

[18] a) See ref.[2b]; b) S. Mosca, Y. Yu, J. V. Gavette, K.-D. Zhang, J. Rebek Jr., *J. Am. Chem. Soc.* **2015**, *137*, 14582–14583; c) See ref.[2c]; d) T. Iwasawa, R. J. Hooley, J. Rebek Jr., *Science* **2007**, *317*, 493–496.

[19] M. P. Schramm, M. Kanaura, K. Ito, M. Ide, T. Iwasawa, *Eur. J. Org. Chem.* **2016**, *2016*, 813–820.

[20] a) R. Bellini, S. H. Chikkali, G. Berthon-Gelloz, J. N. H. Reek, *Angew. Chem. Int. Ed.* **2011**, *50*, 7342–7345; *Angew. Chem.* **2011**, *123*, 7480; b) V. Bocokic, A. Kalkan, M. Lutz, A. L. Spek, D. T. Gryko, J. N. H. Reek, *Nat. Commun.* **2013**, *4*, No. 2670; c) M. Jouffroy, R. Gramage-Doria, D. Armspach, D. Sémeril, W. Oberhauser, D. Matt, L. Toupet, *Angew. Chem. Int. Ed.* **2014**, *53*, 3937–3940; *Angew. Chem.* **2014**, *126*, 4018.

[21] a) D. Sémeril, C. Jeunesse, D. Matt, L. Toupet, *Angew. Chem. Int. Ed.* **2006**, *45*, 5810–5814; *Angew. Chem.* **2006**, *118*, 5942; b) D. Sémeril, D. Matt, L. Toupet, *Chem. Eur. J.* **2008**, *14*, 7144–7155; c) D. Sémeril, D. Matt, L. Toupet, W. Oberhauser, C. Bianchini, *Chem. Eur. J.* **2010**, *16*, 13843–13849.

[22] a) M. E. Broussard, B. Juna, S. G. Train, W.-J. Peng, S. A. Laneman, G. G. Stanley, *Science* **1993**, *260*, 1784–1788; b) D. A. Aubry, N. N. Bridges, K. Ezell, G. G. Stanley, *J. Am. Chem. Soc.* **2003**, *125*, 11180–11181; c) D. G. H. Hetterscheid, S. H. Chikkali, B. de Bruin, J. N. H. Reek, *ChemCatChem* **2013**, *5*, 2785–2793.

Received: July 20, 2019